lubricants
Article

The Tribological Properties of Multi-Layered Graphene as Additives of PAO2 Oil in Steel–Steel Contacts

Yan-Bao Guo * and Si-Wei Zhang *
College of Mechanical and Transportation Engineering, China University of Petroleum, Beijing 102249, China
***** Correspondence: gyb@cup.edu.cn (Y.-B.G.); swzhang99@sina.com (S.-W.Z.);
Tel.: +86-10-89733727 (Y.-B.G.); +86-10-62396260 (S.-W.Z.)
Academic Editor: Robert J. K. Wood
Received: 29 May 2016; Accepted: 29 August 2016; Published: 31 August 2016
Abstract: Multi-layered graphene was prepared by supercritical CO_2 exfoliation of graphite. As the additives of polyalphaolefin-2 (PAO2) oil, its tribological properties were investigated using four-ball test method. The friction reduction and anti-wear ability of pure lubricant was improved by the addition of graphene. With a favorable concentration, the graphene was dispersive. The PAO2 oil with 0.05 wt % graphene showed better tribological properties than that for the other concentration of graphene additives. It could be used as a good lubricant additive for its excellent tribological characteristics, and the multi-layered graphene can bear the load of the steel ball and prevent direct contact of the mating metal surfaces. However, a higher concentration would cause the agglomeration of graphene and weaken the improvement of tribological properties.
Keywords: graphene; additives; PAO2; lubrication; tribological properties

1. Introduction

Friction and wear remain the primary modes of mechanical energy dissipation in moving mechanical assemblies [1]. Sliding, rolling, and rotating contact interfaces in every artificial, natural, and biological system can generate friction. If friction is not controlled or reduced, it often causes greater wear losses and, hence, shorter life and poor reliability [2]. The most effective way to control friction is to use a lubricant in liquid or solid forms. Thus, the major demand for low-friction and long-life of mechanical assemblies is satisfied for purposes of energy saving, emission reduction, and environmental protection. Green tribology is emphasized in environmentally friendly energy and materials, as well as the enhancement of the environment and the quality of life [3–5].

As is well known, lubrication is an important measure to reduce friction and wear in many engineering fields. There are two kinds of liquid lubricants, namely water-based and oil-based. The oil-based lubricants are generally used in most areas due to its many advantages, such as its wide sources, high thermal conductivity, etc. [6]. In recent years, the anti-friction and wear additives are usually used to improve the tribological behaviors of lubricants at low concentrations, especially for the environmentally friendly lubricants [7]. Low-dimensional nanomaterials with self-lubricating capability (such as MoS_2, WS_2, graphite, carbon nanotubes, and so on) might be considered as potential low-friction and anti-wear additives for future engine oil application owing to their unique size, shape, chemistry, and structure morphology. Recently, Erdemir [8] reviewed the latest research trends in 0 to 3D self-lubricating nanomaterials as potential oil additives and their prospects for commercial applications. He concluded that self-lubricating nanomaterials with 0 to 3D structural architectures may hold great promise for further enhancing the friction reducing, anti-wear, and anti-scuffing performance of future lubricating oil.

Graphene, a promising material with 2D laminated structure, has attracted considerable attention since its discovery [9,10]. In recent years, graphene has played important roles in many fields due to its

amazing mechanical, optical, and electronic properties [11–13]. There are several methods to prepare graphene, such as redox process [14], micro-mechanical stripping method [9], SiC epitaxial growth method, and chemical vapor deposition (CVD) [15]. A potentially useful method of supercritical carbon dioxide ($SCCO_2$) exfoliation of graphite was used to provide less-damaged graphene sheets [16], and this technique offers a low-cost, simple approach to large-scale production of pure graphene sheets without the need for complicated processing steps or chemical treatment [17].

With the development of carbon nanomaterials, nanoplatelet-structural graphene as a lubricant additive has gained wide attention [18–20]. Song and coworkers have found that oxide graphene

nanosheets show better tribological properties than oxide multiwall carbon nanotubes (CNTs– COOH) in aqueous medium [21]. The performance of graphene oxide dispersions in water contacting diamond-like carbon and stainless steel were studied, and the tribological mechanism of graphene oxide additives in water was presented [22]. In addition, the compound lubricants containing graphene as an additive is a promising measure in the lubrication domain. Min et al. [23] investigated the polyimide (PI)/graphene oxide (GO) nanocomposite films and their tribological behaviors under seawater lubrication, which could effectively transfer load between the contact surfaces. Some researchers have reported the tribological behavior of graphene oxide nanosheets in mineral oil for boundary and mixed lubrication, and showed the relationship between protective film and the frictional coefficient trend in the boundary regime [24]. Eswaraiah et al. [25] investigated the friction reduction behavior and anti-wear performance of ultrathin graphene (UG) prepared by exfoliation of graphite oxide by a novel technique based on focused solar radiation, and pointed out the importance of forming nanobearings in reducing the friction and wear. Furthermore, graphene nanoflakes as an addition to grease are usefulness for decreasing the coefficient of friction and wear of friction pairs [26,27]. In order to make graphene homogeneously dispersed, some measures were taken. Investigators reported a study on friction and wear performance when graphene sheets were modified by oleic acid as additives to lubricant oils [28]. More recently, a series of calcium borate/graphene oxide (CB/GO) and Cu/reduced graphene oxide composites were synthesized, which indicated that the formation of an interfacial boundary lubrication layer improved friction and wear properties [13,29]. Recent studies in the nano- and macroscale have shown graphene to have the potential to substantially lower friction and wear under specific conditions [1]. As lubrication additives, the graphene and graphene oxide are modified. However, mass production of graphene as lubrication additive at engineering scales has yet to be demonstrated for a better prospect of application. Therefore, the aim of this study is to investigate the tribological properties and to reveal the lubrication mechanism of multi-layered graphene (prepared by supercritical CO_2 exfoliation of graphite) as lubrication additives in polyalphaolefin-2 oil (PAO2) in order to assess the application prospect.

2. Experiments

2.1. Materials

The multi-layered graphene was supplied by the State Key Laboratory of Heavy Oil Processing at China University of Petroleum, Beijing. It was prepared by shear-assisted supercritical CO_2 exfoliation (SSCE) process [30], which can produce high-quality and large-quantity graphene nanosheets. Furthermore, the graphene synthesized by SSCE method consists of 90% exfoliated sheets with less than 10 layers and about 70% that have between 5 and 8 layers; this was clearly shown in Yi Liu's research [31]. The scanning electron microscope (SEM) image of graphene is shown in Figure 1. It can be seen that the diameter of the particle is about 10 _m.

Lubricants **2016**, *4*, 30 3 of 12

Figure 1. Scanning electron microscope (SEM) image of grapheme.

The lubricant oil, polyalphaolefin-2 (PAO2), with a viscosity of 2 mPa·s at 40 °C was supplied by Beijing Yanshan Petrochemical Co., Ltd. (Beijing, China). The graphene, without further treatment, was added into pure PAO2. The mixed solutions (three lubricant samples) containing several different concentrations of graphene were ultrasonicated for 30 min before each test. Hereinafter, the four samples in this study are expressed as: 0.0 wt % (pure PAO2), 0.05 wt %, 0.1 wt %, and 0.5 wt %. Graphene can be easily dispersed without any surface modification or surfactant in the oil-based lubricants after ultrasonication, as shown in Figure 2b–d. Furthermore, digital pictures taken 2 weeks after ultrasonication of the different concentration are shown in Figure 2e–g. For the samples just ultrasonicated, it can be noticed that the multi-layered graphene can be dispersed in PAO2. In can be seen that the multi-layered graphene can be easily dispersed without surface modification or surfactant in the oil-based lubricants, as shown in Figure 2b–d, after ultrasonication. At low concentration, the graphene particles are uniformly dispersed, and as time passes, the particles gradually aggregate and precipitate at a low speed. However, as shown in Figure 2f,g, with a higher graphene concentration, the graphene particles easily assemble and become high-weight particle groups which are easily precipitated for the gravity effect. The dispersions displayed only short-term stability and precipitated completely after a few weeks. Comparing the different concentrations, increasing graphene concentration increased the precipitation rate. This is due to the aggregation of particles at a higher concentration.

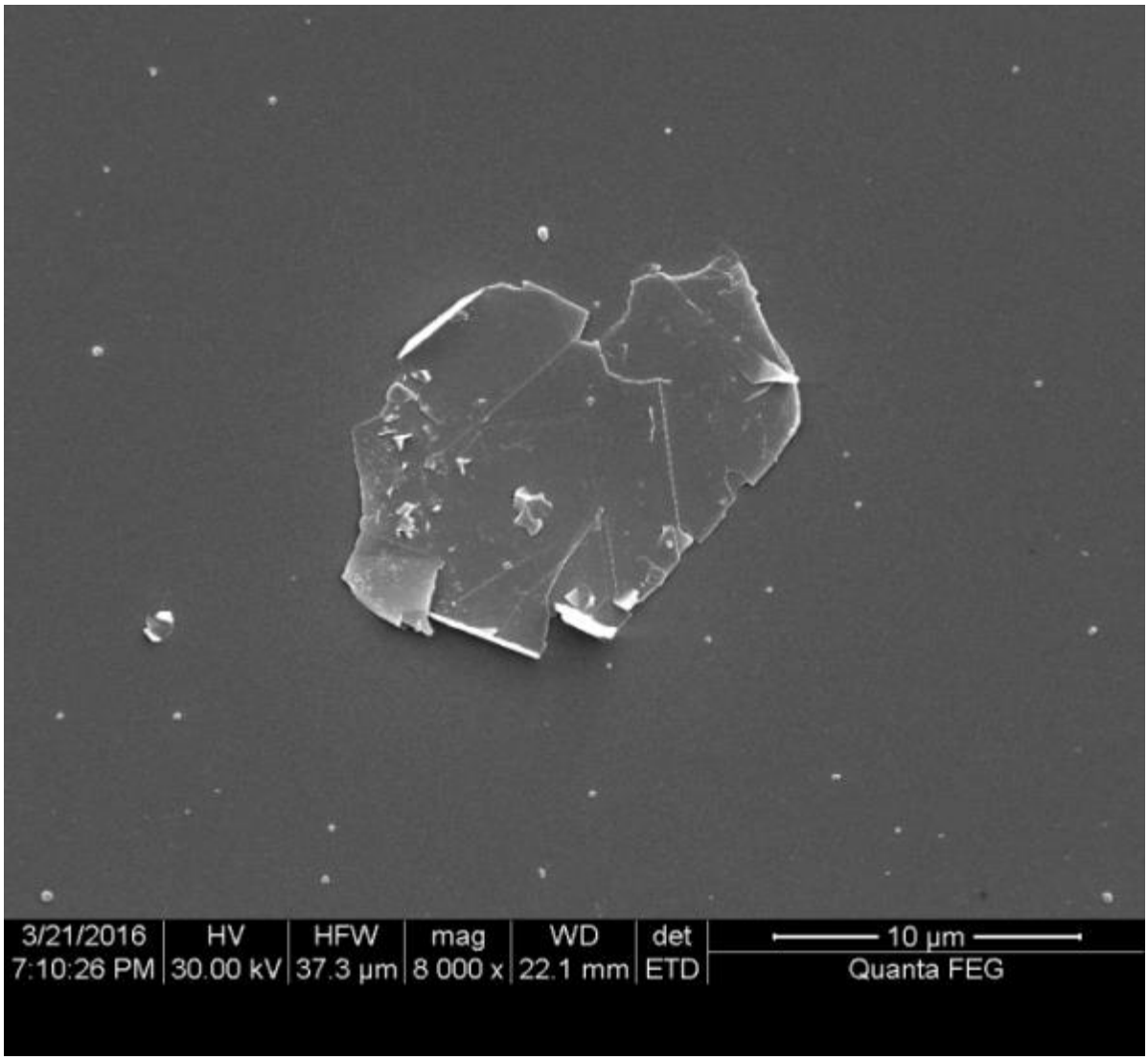

Figure 1. Scanning electron microscope (SEM) image of grapheme.

The lubricant oil, polyalphaolefin-2 (PAO2), with a viscosity of 2 mPa_s at 40 _C was supplied by Beijing Yanshan Petrochemical Co., Ltd. (Beijing, China). The graphene, without further treatment, was added into pure PAO2. The mixed solutions (three lubricant samples) containing several different concentrations of graphene were ultrasonicated for 30 min before each test. Hereinafter, the four samples in this study are expressed as: 0.0 wt % (pure PAO2), 0.05 wt %, 0.1 wt %, and 0.5 wt %. Graphene can be easily dispersed without any surface modification or surfactant in the oil-based lubricants after ultrasonication, as shown in Figure 2b–d. Furthermore, digital pictures taken 2 weeks after ultrasonication of the different concentration are shown in Figure 2e–g. For the samples just ultrasonicated, it can be noticed that the multi-layered graphene can be dispersed in PAO2. In can be seen that the multi-layered graphene can be easily dispersed without surface modification or surfactant in the oil-based lubricants, as shown in Figure 2b–d, after ultrasonication. At low concentration, the graphene particles are uniformly dispersed, and as time passes, the particles gradually aggregate and precipitate at a low speed. However, as shown in Figure 2f,g, with a higher graphene concentration, the graphene particles easily assemble and become high-weight particle groups which are easily precipitated for the gravity effect. The dispersions displayed only short-term stability and precipitated completely after a few weeks. Comparing the different concentrations, increasing graphene concentration increased the precipitation rate. This is due to the aggregation of

particles at a higher concentration.

2.2. Instruments and Experimental Parameters

The frictional coefficient, wear scar tests of multi-layered graphene as additives of PAO2 were evaluated by a multispecimen test machine (FALEX tribology 1506, USA) with a four-ball configuration. The tester was operated with one steel ball under load rotating against three steel balls held stationary in the form of a cradle. Before operating the machine with the test balls, the components were cleaned with petroleum ether under ultrasonication, rinsed with alcohol, and finally dried with a stream of nitrogen. Steel balls—made of AISI-52100 steel with a diameter of 12.7 mm and a hardness of 64~66 HRC—were used in the four-ball test. Before and after each test, the steel balls were cleaned in petroleum ether and absolute ethyl alcohol with ultrasonication, respectively. Then, the samples

were dried with a stream of nitrogen. Three 12.7 mm diameter steel balls were clamped together and covered with pure PAO2 or graphene-added PAO2 lubricants to be evaluated. The experimental set u*Lu*p*br*o*ic*f*an*th*t*s*e **20t1r6**ib, *4*o,m 30e ter is shown in Figure 3 along with schematic view of the four-ball assembly.

Figure 2. Digital pictures of pure polyalphaolefin-2 oil (PAO2) (**a**); and with different concentrations of graphene additives: 0.05 wt % (**b**); 0.1 wt % (**c**); and 0.5 wt % (**d**). After 2 weeks, the pictures of 0.05 wt %, 0.1 wt %, and 0.5 wt % are shown in (**e**), (**f**), and (**g**), respectively.

2.2. Instruments and Experimental Parameters

The frictional coefficient, wear scar tests of multi-layered graphene as additives of PAO2 were evaluated by a multispecimen test machine (FALEX tribology 1506, USA) with a four-ball configuration. The tester was operated with one steel ball under load rotating against three steel balls held stationary in the form of a cradle. Before operating the machine with the test balls, the components were cleaned with petroleum ether under ultrasonication, rinsed with alcohol, and finally dried with a stream of nitrogen. Steel balls—made of AISI-52100 steel with a diameter of 12.7 mm and a hardness of 64~66 HRC—were used in the four-ball test. Before and after each test, the steel balls were cleaned in petroleum ether and absolute ethyl alcohol with ultrasonication, respectively. Then, the samples were dried with a stream of nitrogen. Three 12.7 mm diameter steel balls were clamped together and covered with pure PAO2 or graphene-added PAO2 lubricants to be evaluated. The experimental set up of the tribometer is shown in Figure 3 along with schematic view of the four-ball assembly.

Figure 3. Schematic view of the four-ball assembly.

Figure 2. Digital pictures of pure polyalphaolefin-2 oil (PAO2) (**a**); and with different concentrations of graphene additives: 0.05 wt % (**b**); 0.1 wt % (**c**); and 0.5 wt % (**d**). After 2 weeks, the pictures of 0.05 wt %, 0.1 wt %, and 0.5 wt % are shown in (**e**), (**f**), and (**g**), respectively.

Figure 2. Digital pictures of pure polyalphaolefin-2 oil (PAO2) (**a**); and with different concentrations of graphene additives: 0.05 wt % (**b**); 0.1 wt % (**c**); and 0.5 wt % (**d**). After 2 weeks, the pictures of 0.05 wt %, 0.1 wt %, and 0.5 wt % are shown in (**e**), (**f**), and (**g**), respectively.

2.2. Instruments and Experimental Parameters

The frictional coefficient, wear scar tests of multi-layered graphene as additives of PAO2 were evaluated by a multispecimen test machine (FALEX tribology 1506, USA) with a four-ball configuration. The tester was operated with one steel ball under load rotating against three steel balls held stationary in the form of a cradle. Before operating the machine with the test balls, the components were cleaned with petroleum ether under ultrasonication, rinsed with alcohol, and finally dried with a stream of nitrogen. Steel balls—made of AISI-52100 steel with a diameter of 12.7 mm and a hardness of 64~66 HRC—were used in the four-ball test. Before and after each test, the steel balls were cleaned in petroleum ether and absolute ethyl alcohol with ultrasonication, respectively. Then, the samples were dried with a stream of nitrogen. Three 12.7 mm diameter steel balls were clamped together and covered with pure PAO2 or graphene-added PAO2 lubricants to be evaluated. The experimental set up of the tribometer is shown in Figure 3 along with schematic view of the four-ball assembly.

FFiigguurree 33.. SScchheemmaattiicc vviieeww ooff tthhee ffoouurr--bbaallll aassssseemmbbllyy..

The effects of load and rotation speed on the lubricants of graphene additives were studied under different loads in the range 120–400 N, and different rotation speeds ranging from 100 rpm up to 400 rpm. In this study, each test was carried out twice under the above condition. New balls were used in every test, and all the tests were conducted at room temperature with a relative humidity of 25%.

In order to characterize the morphology of the scar surface, after the test, the worn scars were detected using scanning electric microscopy (SEM, FEI QUANTA 200F), energy dispersive spectroscopy

(EDS), and 3D white light interference (WLI). Besides, the viscosity of lubrication was measured using an MCR301 rotary rheometer, varying the shear rate from 1 s□1 to 10,000 s□1.

3. Results and Discussion

3.1. Coefficients of Friction (COF)

The COF curves of lubricants with different graphene concentrations (wt %) under load of 120 N and rotation speed of 250 rpm are shown in Figure 4. It can be seen that the fluctuation of COF curves is gentle. Moreover, the values of COF decrease smoothly with the passage of time and are less than that of the pure lubricant. This shows that the graphene has obvious anti-friction properties. The lowest value of COF is found when the graphene concentration is 0.05 wt %, about 78% less than that of pure lubricant.

curves is gentle. Moreover, the values of COF decrease smoothly with the passage of time and are less than that of the pure lubricant. This shows that the graphene has obvious anti-friction properties. The lowest value of COF is found when the graphene concentration is 0.05 wt %, about 78% less than that of pure lubricant.

Figure 5 shows the curves of average COF of different samples under different loads and a rotation speed of 250 rpm, along with the error bars denoting the standard deviation around the rolling mean. It was found that the COF increased with the loads from 120 N up to 400 N for the four samples. Furthermore, when the loads are below 240 N, the COF rises markedly with increasing loading force, and is then stable with increasing load. Furthermore, the COF of the samples under a series of rotation speeds from 100 rpm to 400 rpm with 120 N (Figure 6) shows that the COF of the sample with 0.05 wt % graphene has the lowest friction under different rotation speeds. A comparison among the four samples (PAO2 with different graphene concentrations) shows that reduction of the friction coefficient for the sample with graphene is remarkable (Figures 5 and 6). Additionally, as can be seen from Figure 6, the COF is decreasing with increasing rotation speeds, from 100 rpm to 400 rpm. From the friction curves, it is found that the lubrication regime is mainly boundary and mixed lubrication, and the friction coefficient decreases with increasing sliding speed [24]. In addition, for the graphene-added PAO2, more graphene would be entrained into the rubbing surfaces with the increasing of rotation speed. Moreover, the higher rotation speed is beneficial to the dispersibility of graphene in PAO2 and hinders the precipitation phenomenon.

Figure 4. Friction coefficient curves of different additive concentrations of graphene in PAO2 (load 120 N, rotation speed 250 rpm).

Figure 4. Friction coefficient curves of different additive concentrations of graphene in PAO2 (load 120 N, rotation speed 250 rpm).

Figure 5 shows the curves of average COF of different samples under different loads and a rotation speed of 250 rpm, along with the error bars denoting the standard deviation around the rolling mean. It was found that the COF increased with the loads from 120 N up to 400 N for the four samples. Furthermore, when the loads are below 240 N, the COF rises markedly with increasing loading force, and is then stable with increasing load. Furthermore, the COF of the samples under a series of rotation speeds from 100 rpm to 400 rpm with 120 N (Figure 6) shows that the COF of the sample with 0.05 wt % graphene has the lowest friction under different rotation speeds. A comparison among the four samples (PAO2 with different graphene concentrations) shows that reduction of the friction coefficient for the sample with graphene is remarkable (Figures 5 and 6). Additionally, as can be seen from Figure 6, the COF is decreasing with increasing rotation speeds, from 100 rpm to 400 rpm. From the friction curves, it is found that the lubrication regime is mainly boundary and mixed lubrication, and the friction coefficient decreases with increasing sliding speed [24]. In addition, for the graphene-added PAO2, more graphene would be entrained into the rubbing surfaces with the increasing of rotation speed. Moreover, the higher rotation speed is beneficial to the dispersibility of graphene in PAO2 and hinders the precipitation phenomenon.

Figure 5. Friction coefficients versus different loads (rotation speed of 250 rpm).
Figure 6. Coefficients of friction (COF) of different rotation speeds for different concentrations of graphene additive (load of 120 N).

3.2. Anti-Wear Behaviors

Wear scar diameter (WSD) is a key parameter to evaluate the anti-wear properties of the lubricants. The surface topographies of worn steel balls were investigated by 3D white light interference and the average WSDs were calculated from the surface topography. Figure 7 shows the average WSDs of ball samples under applied load of 120 N and rotation speed of 250 rpm with friction time of 30 min. It can be seen that the average WSD of pure lubricant is about 0.77 mm, which is larger than that of the other three samples. Figure 8 shows the 3D surface images of wear scars of different samples. As shown in Figure 8a, the worn surface in pure lubricant is rough with many wide and deep furrows, but the surface images of the other three samples are smooth except for a few scratches. This wear protective effect is attributed to increased tendency to form a protective film with graphene. The sample with 0.05 wt % graphene has a lower surface roughness than the pure lubricant. In contrast, when 0.5 wt % graphene was added, a number of scratches emerged on the surface with a greater surface roughness. Figure 8e,f shows the linear roughness curve. When 0.05 wt % of graphene was added, the reduction of the WSD is up to 16%. This result indicates that the addition of graphene could improve the anti-wear properties of the lubricants. This might be due to the present of graphene on the friction surface. However, when the concentration increases, the WSD becomes a little larger, perhaps due to abrasive wear occurring [28].

Lubricants **2016**, *4*, 30 6 of 12
Figure 5. Friction coefficients versus different loads (rotation speed of 250 rpm).
Figure 6. Coefficients of friction (COF) of different rotation speeds for different concentrations of
3.2. Anti-Wear Behaviors
Wear scar diameter (WSD) is a key parameter to evaluate the anti-wear properties of the lubricants. The surface topographies of worn steel balls were investigated by 3D white light interference and the average WSDs were calculated from the surface topography. Figure 7 shows the average WSDs of ball samples under applied load of 120 N and rotation speed of 250 rpm with friction time of 30 min. It can be seen that the average WSD of pure lubricant is about 0.77 mm, which is larger than that of the other three samples. Figure 8 shows the 3D surface images of wear scars of different samples. As shown in Figure 8a, the worn surface in pure lubricant is rough with many wide and deep furrows, but the surface images of the other three samples are smooth except for a few scratches. This wear protective effect is attributed to increased tendency to form a protective film with graphene. The sample with 0.05 wt % graphene has a lower surface roughness than the pure lubricant. In contrast, when 0.5 wt % graphene was added, a number of scratches emerged on the surface with a greater surface roughness. Figure 8e,f shows the linear roughness curve. When 0.05 wt % of graphene was added, the reduction of the WSD is up to 16%. This result indicates that the addition of graphene could improve the anti-wear properties of the lubricants. This might be due to the present of graphene on the friction surface. However, when the concentration increases, the WSD becomes a little larger, perhaps due to abrasive wear occurring [28].
graphene additive (load of 120 N).

3.2. Anti-Wear Behaviors

Wear scar diameter (WSD) is a key parameter to evaluate the anti-wear properties of the lubricants. The surface topographies of worn steel balls were investigated by 3D white light interference and the average WSDs were calculated from the surface topography. Figure 7 shows the average WSDs of ball samples under applied load of 120 N and rotation speed of 250 rpm with friction time of 30 min. It can be seen that the average WSD of pure lubricant is about 0.77 mm, which is larger than that of the other three samples. Figure 8 shows the 3D surface images of wear scars of different samples. As shown in Figure 8a, the worn surface in pure lubricant is rough with many wide and deep furrows, but the surface images of the other three samples are smooth except for a few scratches. This wear protective effect is attributed to increased tendency to form a protective film with graphene. The sample with 0.05 wt % graphene has a lower surface roughness than the pure lubricant. In contrast, when 0.5 wt % graphene was added, a number of scratches emerged on the surface with a greater surface roughness. Figure 8e,f shows the linear roughness curve. When 0.05 wt % of graphene was added, the reduction of the WSD is up to 16%. This result indicates that the addition of graphene could improve the anti-wear properties of the lubricants. This might be due to the present of graphene

on the friction surface. However, when the concentration increases, the WSD becomes a little larger, perhaps due to abrasive wear occurring [28].

Figure 7. Wear scar diameter (WSD) of different concentrations of graphene additive (load 120 N, rotation speed 250 rpm).

Figure 8. 3D optical micrographs of the abraded surface with pure PAO2 (**a**); 0.05 wt % (**b**); 0.1 wt % (**c**); 0.5 wt % (**d**) of graphene; linear roughness with (**e**) 0.05 wt % graphene in PAO2 and (**f**) 0.5 wt % graphene in PAO2, respectively.

(**a**) (**b**)
(**c**) (**d**)
(**e**) (**f**)

Figure 7. Wear scar diameter (WSD) of different concentrations of graphene additive (load 120 N, rotation speed 250 rpm).

Figure 7. Wear scar diameter (WSD) of different concentrations of graphene additive (load 120 N, rotation speed 250 rpm).

Figure 8. 3D optical micrographs of the abraded surface with pure PAO2 (**a**); 0.05 wt % (**b**); 0.1 wt % (**c**); 0.5 wt % (**d**) of graphene; linear roughness with (**e**) 0.05 wt % graphene in PAO2 and (**f**) 0.5 wt % graphene in PAO2, respectively.

(**a**) (**b**)
(**c**) (**d**)
(**e**) (**f**)

Figure 8. 3D optical micrographs of the abraded surface with pure PAO2 (**a**); 0.05 wt % (**b**); 0.1 wt % (**c**); 0.5 wt % (**d**) of graphene; linear roughness with (**e**) 0.05 wt % graphene in PAO2 and (**f**) 0.5 wt % graphene in PAO2, respectively.

3.3. Lubrication Mechanism

As stated above, with the addition of graphene additives in PAO2 is effective on the anti-friction and wear-resistant properties. It is well known that the rheological behavior is a key parameter of lubricants [32]. In order to investigate the effect of graphene additives on the rheological behavior of PAO2, the viscosity of samples was measured at 20 _C using a MCR301 rotary rheometer (Figure 9). It was found that the reduction of viscosity was the result of increasing shear rate for all samples. This can be explained by a shear-thinning phenomenon of the base liquids, and the addition of graphene does not change the characteristics of non-Newtonian liquid. Added to this, the addition of graphene causes a slight increase of the viscosity compared with pure PAO2, shown in the illustration insert in Figure 9. This indicated that the viscosity of the four samples were about the same.

3.3. Lubrication Mechanism

As stated above, with the addition of graphene additives in PAO2 is effective on the anti-friction and wear-resistant properties. It is well known that the rheological behavior is a key parameter of lubricants [32]. In order to investigate the effect of graphene additives on the rheological behavior of PAO2, the viscosity of samples was measured at 20 °C using a MCR301 rotary rheometer (Figure 9). It was found that the reduction of viscosity was the result of increasing shear rate for all samples. This can be explained by a shear-thinning phenomenon of the base liquids, and the addition of graphene does not change the characteristics of non-Newtonian liquid. Added to this, the addition of graphene causes a slight increase of the viscosity compared with pure PAO2, shown in the illustration insert in Figure 9. This indicated that the viscosity of the four samples were about the same.

Figure 9. Viscosity of PAO2 solutions with different concentrations of grapheme.

Biphase (solid–liquid) lubricant could be helpful for better explaining the above. It is well known that liquid lubricants can reduce friction by preventing sliding contact interfaces from severe or more frequent metal-to-metal contacts or by forming a low-shear, high-durability film on rubbing surfaces. Depending on the sliding speed/rotation speed and other operating conditions, the lubricant can effectively separate the contacting surfaces and, thereby, reduce the direct metal-to-metal contact and thus friction and wear. In this study, if and when there is metal-to-metal contact, the graphene additives in PAO2 can form a protective film to provide additional safety. According with the Stribeck curve, the lubrication form is mainly mixed lubrication. When the concentration of graphene is appropriate, the favorable dispersive graphene additives into the base lubricant could be beneficial

for the formation of lubrication film and persistence of additives on the rubbing surfaces. However, with the further increase of concentration of graphene, it is too difficult for the graphene additives to enter the rubbing surfaces due to the agglomeration of graphene. Moreover, it also reduces the dispersive behavior of graphene additive.

In this work, it has been shown that under a certain condition of multi-layered graphene, good anti-wear ability has been obtained, and at the same time, a very low friction coefficient is reached. The SEM and EDS of surface morphologies of three samples (0.0 wt %, 0.05 wt %, and 0.5 wt %) are shown in Figure 10a–c, respectively. In contrast, the rubbing surfaces of 0.0 wt % and 0.5 wt % have wide and deep furrows. Besides, some pits and spalls are non-uniformly covered on the surfaces. Furthermore, some coating (black region) appeared on the abraded surface as shown in Figure 10b,c. Especially for the sample with 0.05 wt % graphene, the region of coating extended as shown in Figure 10b. As presented in Figure 10b, the rubbing surface lubricated with PAO2 added 0.05 wt % multilayered graphene is smoother. Thus, the mechanism of the reducing friction and anti-wear of graphene particles dispersed in PAO2 can be confirmed by results of SEM. As seen from Figure 10a–c, the carbon content in the rubbed surface of the sample with 0.05 wt % graphene is the highest. Taking Viscosity Biphase (solid–liquid) lubricant could be helpful for better explaining the above. It is well known that liquid lubricants can reduce friction by preventing sliding contact interfaces from severe or more frequent metal-to-metal contacts or by forming a low-shear, high-durability film on rubbing surfaces. Depending on the sliding speed/rotation speed and other operating conditions, the lubricant can effectively separate the contacting surfaces and, thereby, reduce the direct metal-to-metal contact and thus friction and wear. In this study, if and when there is metal-to-metal contact, the graphene additives in PAO2 can form a protective film to provide additional safety. According with the Stribeck curve, the lubrication form is mainly mixed lubrication. When the concentration of graphene is appropriate, the favorable dispersive graphene additives into the base lubricant could be beneficial for the formation of lubrication film and persistence of additives on the rubbing surfaces. However, with the further increase of concentration of graphene, it is too difficult for the graphene additives to enter the rubbing surfaces due to the agglomeration of graphene. Moreover, it also reduces the dispersive behavior of graphene additive.

In this work, it has been shown that under a certain condition of multi-layered graphene, good anti-wear ability has been obtained, and at the same time, a very low friction coefficient is reached. The SEM and EDS of surface morphologies of three samples (0.0 wt %, 0.05 wt %, and 0.5 wt %) are shown in Figure 10a–c, respectively. In contrast, the rubbing surfaces of 0.0 wt % and 0.5 wt % have wide and deep furrows. Besides, some pits and spalls are non-uniformly covered on the surfaces. Furthermore, some coating (black region) appeared on the abraded surface as shown in Figure 10b,c. Especially for the sample with 0.05 wt % graphene, the region of coating extended as shown in Figure 10b. As presented in Figure 10b, the rubbing surface lubricated with PAO2 added 0.05 wt % multi-layered graphene is smoother. Thus, the mechanism of the reducing friction and anti-wear of graphene particles dispersed in PAO2 can be confirmed by results of SEM. As seen from Figure 10a–c,

the carbon content in the rubbed surface of the sample with 0.05 wt % graphene is the highest. Taking into account the fact that graphene is made of carbon, it can be deduced that the graphene content in contact surfaces of this sample is also the highest. This indicates that a thin tribofilm is formed on the metal surface. The tribofilms could not only bear the load of the steel ball, but also prevent the direct contact of two mating metal surfaces [21]. Therefore, the anti-wear ability of the PAO2 with graphene additives was improved, and the friction coefficient was reduced significantly. However, when the concentration of graphene further increased, the anti-wear and friction-reducing performance was weakened. This might be due to the agglomeration of graphene during the friction process. The SEM images of the sample with 0.5 wt % graphene test are shown in Figure 11. It was observed that the agglomeration of graphene

into account the fact that graphene is made of carbon, it can be deduced that the graphene content in contact surfaces of this sample is also the highest. This indicates that a thin tribofilm is formed on the metal surface. The tribofilms could not only bear the load of the steel ball, but also prevent the direct contact of two mating metal surfaces [21]. Therefore, the anti-wear ability of the PAO2 with graphene additives was improved, and the friction coefficient was reduced significantly. However, when the concentration of graphene further increased, and friction-reducing performance was weakened. This might be due to the agglomeration during the friction process. The SEM

images of the sample with 0.5 wt % graphene after the friction test are shown in Figure 11. It was observed that the agglomeration of graphene appeared obviously.

Figure 10. SEM surface morphologies and energy dispersive spectroscopy (EDS) of the wear scars. (**a**) 0.0 wt % (pure PAO2); (**b**) 0.05 wt %; and (**c**) 0.5 wt % of graphene.

In a real friction process, the contact surfaces were filled with the dispersed graphene, and then graphene sheets in PAO2 on contact surfaces can serve as spacers, preventing some real contact. In addition, the two-dimensional sheet shape of graphene could provide easy shear and more easily a slider between the two contact surfaces. So, the friction coefficient of PAO2 with graphene decreased

Figure 10. SEM surface morphologies and energy dispersive spectroscopy (EDS) of the wear scars. (**a**) 0.0 wt % (pure PAO2); (**b**) 0.05 wt %; and (**c**) 0.5 wt % of graphene.

In a real friction process, the contact surfaces were filled with the dispersed graphene, and then graphene sheets in PAO2 on contact surfaces can serve as spacers, preventing some real contact. In addition, the two-dimensional sheet shape of graphene could provide easy shear and more easily a

slider between the two contact surfaces. So, the friction coefficient of PAO2 with graphene decreased obviously. All the tribological behaviors mentioned above show that graphene is very attractive for demanding tribological applications to achieve low friction and wear regimes.

Results indicated that a thin tribofilm is formed on the metal surface during the friction test. The tribofilms could in some degree bear the load of the steel ball, but also prevent from some direct contact between contact surfaces. Therefore, the anti-wear ability of the PAO2 with graphene additives was improved, and the friction coefficient was reduced significantly. In addition, the rubbing surface lubricated with PAO2 added with multi-layered graphene is smoother than the pure PAO2 lubricant condition.

The friction-reduction ability of multi-layered graphene sheets as lubricant additive could be explained by better dispersion. It could be deduced that the high-concentration graphene presented poor dispersion, with large graphene bundles caused by agglomeration being easily formed in higher concentrations, resulting in the friction coefficient increasing. When the concentration of graphene increases, the agglomeration and shape change of graphene occurs with the friction process, which can be seen from Figure 11; it is difficult for larger additives to enter into the contact area during the rotation friction process. Therefore, the improvement of anti-friction and abrasive properties were weakened with the higher concentration of graphene additives.

obviously. All the tribological behaviors mentioned above show that graphene is very attractive for demanding tribological applications to achieve low friction and wear regimes.

Results indicated that a thin tribofilm is formed on the metal surface during the friction test. The tribofilms could in some degree bear the load of the steel ball, but also prevent from some direct contact between contact surfaces. Therefore, the anti-wear ability of the PAO2 with graphene additives was improved, and the friction coefficient was reduced significantly. In addition, the rubbing surface lubricated with PAO2 added with multi-layered graphene is smoother than the pure PAO2 lubricant condition.

The friction-reduction ability of multi-layered graphene sheets as lubricant additive could be explained by better dispersion. It could be deduced that the high-concentration graphene presented poor dispersion, with large graphene bundles caused by agglomeration being easily formed in higher concentrations, resulting in the friction coefficient increasing. When the concentration of graphene increases, the agglomeration and shape change of graphene occurs with the friction process, which can be seen from Figure 11; it is difficult for larger additives to enter into the contact area during the rotation friction process. Therefore, the improvement of anti-friction and abrasive properties were weakened with the higher concentration of graphene additives.

Figure 11. SEM images of agglomerated graphene after friction test (0.5 wt % concentration).

4. Conclusions

Multi-layered graphene sheets prepared by supercritical CO_2 exfoliation of graphite showed excellent performance of friction reduction and anti-wear as 0.05 wt % additives of PAO2 in steel–steel contacts in comparison with the pure lubricant. With the 0.05 wt % graphene additives, friction coefficient reduced by about 78% and wear scar diameter decreased markedly compared to that of pure PAO2 lubricant under a load of 120 N and rotation speed 250 rpm. The lubrication mechanism was presented, which indicated that the graphene additives with the lubricant entered into the rubbing surfaces, and a thin physical triofilm formed on the rubbing surfaces to prevent the direct

contact of these surfaces. This could explain the improvement of friction and wear properties with the appropriate concentration of graphene additives. The test results show that multi-layered graphene is very attractive for demanding tribological applications to achieve low friction and wear regimes.

Acknowledgments: This research is supported by Beijing Natural Science Foundation (No. 3162024), the National Natural Science Foundation of China (No. 51305459), Tribology Science Foundation of State Key Laboratory of Tribology, Tsinghua University (No. SKLTKF14A08) and the Science Foundation of China University of Petroleum (No. 2462013YJRC032).

Author Contributions: All authors were involved in the preparation and correction of the manuscript.

Conflicts of Interest: The authors declare no conflict of interest.

Conclusions

of friction reduction and anti-wear as 0.05 wt % additives of PAO2 in steel–steel contacts in comparison with the pure lubricant. With the 0.05 wt % graphene additives, presented, which indicated that the graphene additives with the lubricant entered into the rubbing surfaces, and a thin physical triofilm formed on the rubbing surfaces to prevent the direct contact of these surfaces. This could explain the improvement of friction and wear properties with the appropriate concentration of graphene additives. The test results show that multi-layered graphene is very attractive for demanding tribological applications to achieve low friction and wear regimes.

Acknowledgments: This research is supported by Beijing Natural Science Foundation (No. 3162024), the National Natural Science Foundation of China (No. 51305459), Tribology Science Foundation of State Key Laboratory of Tribology, Tsinghua University (No. SKLTKF14A08) and the Science Foundation of China University of Petroleum (No. 2462013YJRC032).

Author Contributions: All authors were involved in the preparation and correction of the manuscript.

Conflicts of Interest: The authors declare no conflict of interest.

References

1. Berman, D.; Deshmukh, S.A.; Sankaranarayanan, S.K.R.S.; Erdemie, A.; Sumant, A.V. Macroscale superlubricity enabled by graphene nanoscroll formation. Science **2015**, 348, 1118–1122. [CrossRef] [PubMed]
2. Berman, D.; Erdemir, A.; Sumant, A.V. Graphene: A new emerging lubricant. Mater. Today **2014**, 17, 31–42. [CrossRef]
3. Zhang, S.W. Green tribology—The way forward to a sustainable society. In Proceedings of the International Tribology Congress—ASIATRIB, Perth, Australia, 5–9 December 2010; Volume 6.
4. Zhang, S.W. Green tribology: Fundamentals and future development. Friction **2013**, 1, 186–194. [CrossRef]
5. Zhang, S.W. Recent developments of green tribology. Surface Topogr. Metrol. Prop. **2016**, 4, 023004. [CrossRef]
6. Totten, G.E. Handbook of Hydraulic Fluid Technology; CRC Press: Boca Raton, FL, USA, 2011.
7. Adhvaryu, A.; Erhan, S.Z.; Perez, J.M. Tribological studies of thermally and chemically modified vegetable oils for use as environmentally friendly lubricants. Wear **2004**, 257, 359–367. [CrossRef]
8. Erdemir, A. Advances In novel nanolubrication additives for improved friction and wear properties. In Proceedings of the 5th World Tribology Congress, Torino, Italy, 8–13 September 2013.
9. Novoselov, K.S.; Geim, A.K.; Morozov, S.V.; Jiang, D.; Zhang, Y.; Dubonos, S.V.; Grigorieva, I.V.; Firsov, A.A. Electric field effect in atomically thin carbon films. Science **2004**, 306, 666–669. [CrossRef] [PubMed]
10. Nair, R.R.; Blake, P.; Grigorenko, A.N.; Novoselov, K.S.; Booth, T.J.; Stauber, T.; Peres, N.M.R.; Geim, A.K. Fine structure constant defines visual transparency of graphene. Science **2008**, 320, 1308. [CrossRef] [PubMed]
11. Lee, C.; Wei, X.D.; Kysar, J.W.; Hone, J. Measurement of the elastic properties and intrinsic strength of monolayer graphene. Science **2008**, 321, 385–388. [CrossRef] [PubMed]
12. Bolotin, K.I.; Sikes, K.J.; Jiang, Z.; Klima, M.; Fudenberg, G.; Hone, J.; Kim, P.; Stormer, H.L. Ultrahigh electron mobility in suspended graphene. Solid State Commun. **2008**, 146, 351–355. [CrossRef]
13. Jia, Z.; Chen, T.; Wang, J.; Ni, J.; Li, H.; Shao, X. Synthesis, characterization and tribological properties of Cu/reduced graphene oxide composites. Tribol. Int. **2015**, 88, 17–24. [CrossRef]
14. Liu, X.W.; Mao, J.J.; Liu, P.D.; Wei, X.W. Fabrication of metal-graphene hybrid materials by electroless deposition. Carbon **2011**, 49, 477–483. [CrossRef]
15. Liu, W.; Chung, C.H.; Miao, C.Q.; Wang, Y.J.; Li, B.Y.; Ruan, L.Y. Chemical vapor deposition of large area few layer graphene on Si catalyzed with nickel films. Thin Solid Films **2010**, 518, S128–S132. [CrossRef]
16. Sim, H.S.; Kim, T.A.; Lee, K.H.; Min, P. Preparation of graphene nanosheets through repeated supercritical carbon dioxide process. Mater. Lett. **2012**, 89, 343–346. [CrossRef]
17. Pu, N.W.; Wang, C.A.; Sung, Y.; Liu, Y.M.; Ger, M.D. Production of few-layer graphene by supercritical CO_2 exfoliation of graphite. Mater. Lett. **2009**, 63, 1987–1989. [CrossRef]
18. Lin, J.S.;Wang, L.W.; Chen, G.H. Modification of graphene platelets and their tribological properties as a lubricant additive. Tribol. Lett. **2011**, 41, 209–215. [CrossRef]
19. Kinoshita, H.; Nishina, Y.; Alias, A.A.; Fujii, M. Tribological properties of monolayer graphene oxide sheets as water-based lubricant additives. Carbon **2014**, 66, 720–723. [CrossRef]

20. Berman, D.; Erdemir, A.; Sumant, A.V. Few layer graphene to ewduce wear and friction on sliding steel surfaces. Carbon **2013**, 54, 454–459. [CrossRef]
21. Song, H.J.; Li, N. Frictional behavior of oxide graphene nanosheets as water-base lubricant additive. Appl. Phys. A Mater. Sci. Process. **2011**, 105, 827–832. [CrossRef]
22. Elomaa, O.; Singh, V.K.; Iyer, A.; Hakala, T.J.; Koskinen, J. Graphene oxide in water lubrication on diamond-like carbon vs. stainless steel high-load contacts. Diam. Relat. Mater. **2015**, 52, 43–48. [CrossRef]
23. Min, C.; Nie, P.; Song, H.J.; Zhang, Z.; Zhao, K. Study of tribological properties of polyimide/graphene oxide nanocomposite films under seawater-lubricated condition. Tribol. Int. **2014**, 80, 131–140. [CrossRef]
24. Senatore, A.; D'Agostino, V.; Petrone, V.; Ciambelli, P.; Sarno, M. Graphene oxide nanosheets as effective friction modifier for oil lubricant: Materials, methods, and tribological results. ISRN Tribol. **2013**, 2013, 425809. [CrossRef]
25. Eswaraiah, V.; Sankaranarayanan, V.; Ramaprabhu, S. Graphene-based engine oil nanofluids for tribological applications. ACS Appl. Mater. Interfaces **2011**, 3, 4221–4227. [CrossRef] [PubMed]
Lubricants **2016**, 4, 30 12 of 12
26. Ju´s, A.; Kami´ nski, M.; Radzikowska-Ju´s, W. Influence of graphene nanoflakes addition on grease tribological properties. In Proceedings of the 22th International Conference on Applied Physics of Condensed Matter, Štrbské Pleso, Slovakia, 22–24 June 2016; pp. 307–310.
27. Missala, T.; Szewczyk, R.; Winiarski, W.; Hamela, M.; Kamin´ ski, M.; Da˛ browski, S.; Pogorzelski, D.; Jakubowska, M.; Tomasik, J. Study on tribological properties of lubricating grease with additive of graphene. In Progress in Automation, Robotics and Measuring Techniques; Springer International Publishing: Berlin/Heidelberg, Germany, 2015; pp. 181–187.
28. Zhang, W.; Zhou, M.; Zhu, H.; Tian, Y.; Wang, K.; Wei, J.; Ji, F.; Li, X.; Li, Z.; Zhang, P.; et al. Tribological properties of oleic acid-modified graphene as lubricant oil additives. J. Phys. D Appl. Phys. **2011**, 44, 205303. [CrossRef]
29. Jia, Z.; Pang, X.; Li, H.; Ni, J.; Shao, X. Synthesis and wear behavior of oleic acid capped calcium borate/graphene oxide composites. Tribol. Int. **2015**, 90, 240–247. [CrossRef]
30. Li, L.; Li, G.H.; Li, Y.F.; Gao, J.S.; Xu, C.M. Preparation of graphene from graphite by supercritical CO_2 exfoliation assisted with fluid shear. Chin. Sci. Bull. **2015**, 60, 2561–2566. (In Chinese) [CrossRef]
31. Li, L.; Xu, J.; Li, G.; Jia, X.; Li, Y.; Yang, F.; Zhang, L.; Xu, C.; Gao, J.; Liu, Y.; et al. Preparation of graphene nanosheets by shear-assisted supercritical CO_2 exfoliation. Chem. Eng. J. **2016**, 284, 78–84. [CrossRef]
32. Xiao, H.; Dai, W.; Kan, Y.; Clearfield, A.; Liang, H. Amine-intercalated _-zirconium phosphates as lubricant additives. Appl. Surface Sci. **2015**, 329, 383–389. [CrossRef]